Taylor & Francis
Taylor & Francis Group

Microwave Photonics for High-Resolution and High-Speed Interrogation of Fiber Bragg Grating Sensors

JIANPING YAO[1]

[1]Microwave Photonics Research Laboratory, School of Electrical Engineering and Computer Science, University of Ottawa, Ottawa, Ontario, Canada

Abstract *Conventional fiber Bragg grating sensors have a few limitations, such as limited interrogation resolution and speed and difficulty in separating different measurands. In this article, microwave photonic techniques applied to fiber Bragg grating sensors to improve the interrogation resolution and speed are discussed. Experimental results to validate the techniques are provided.*

1. Introduction

Fiber Bragg grating (FBG) sensors have been considered a mainstream sensing technology and have been investigated extensively in the last few decades thanks to their intrinsic advantages over conventional sensors, such as compact size, low weight, immunity to electromagnetic interference, and advanced multiplexing and communications capabilities, enabled by the nature of an optical fiber [1]. An FBG-based sensor, either passive or active, is conventionally a wavelength-encoded sensing device, and it typically converts the target measurand, such as strain, temperature, and/or pressure, to a wavelength shift in the spectral response of the device, which is interrogated by use of an optical spectrum analyzer or an optical filter, such as a Fabry-Perot (FP) scanning filter and an optical edge filter. Among these interrogation techniques, the wavelength shift information can be typically acquired by either using an optical spectrum analyzer or an optical scanning filter to directly read the wavelength shift information or an optical edge filter to convert the wavelength shift to a power change. However, for a given spectrum range, when using an optical spectrum analyzer or an optical scanning filter, the higher the sensing resolution is, the more time is required to scan the spectrum range, and the lower the interrogation speed is. The use of an optical edge filter may increase the interrogation speed, but the sensing resolution is limited. Therefore, the first limitation of a conventional FBG sensor is the slow interrogation speed for high-resolution interrogation. A comparison of different
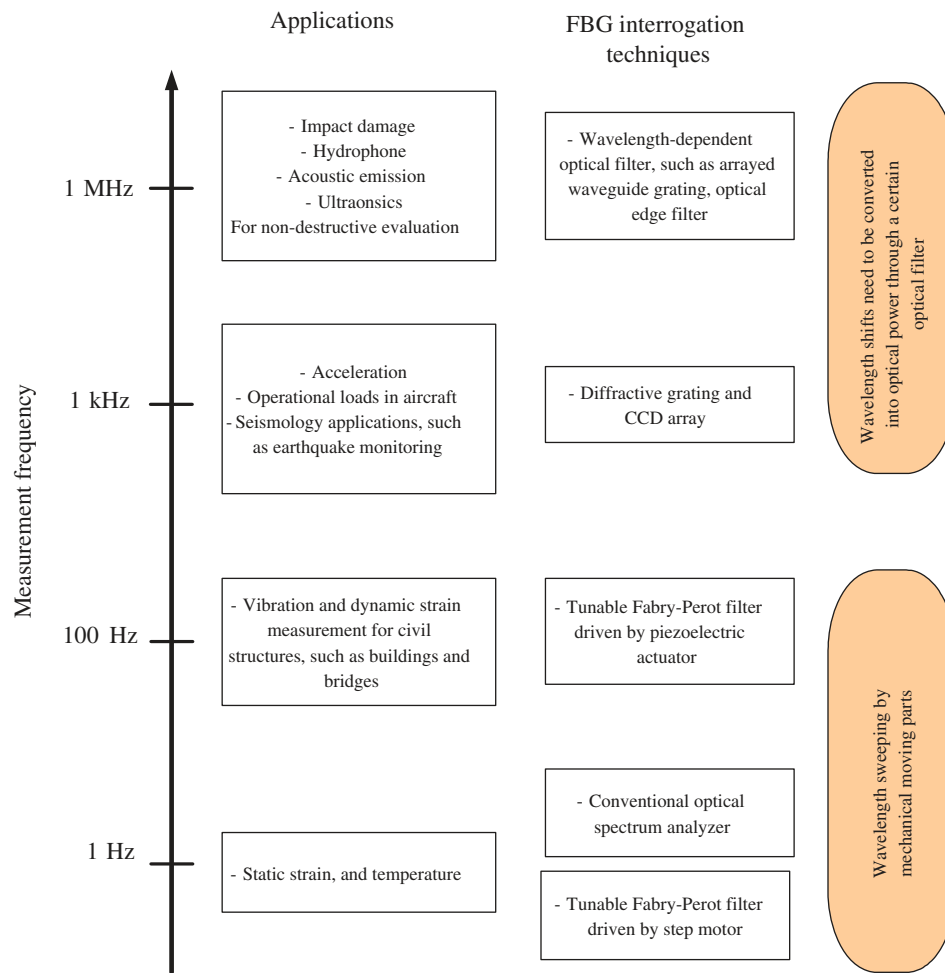
Applications

FBG interrogation techniques

Figure 1. FBG interrogation methods classified by measurement frequency.

FBG interrogation methods with different interrogation speeds is summarized in Figure 1. Another limitation of a conventional FBG sensor is the difficulty in simultaneously distinguishing and measuring multiple target measurands, since most measurands can introduce the same wavelength shift to an FBG. Therefore, additional measures must be taken to separate different measurands. For example, a second FBG [2–5] can be used as a temperature reference to isolate the strain information, but this approach will increase the complexity of the system. Therefore, for practical applications, it is highly desirable that a single FBG is used to perform multiple measurements simultaneously with a high interrogation resolution and speed, in which microwave photonics techniques will play an important role.

Microwave photonics is a field that studies the generation, processing, control, and distributions of microwave signals by means of photonics. The key advantages of manipulating microwave signals in the optical domain are the wideband width and high speed, which may not be achievable by digital electronics. For sensing applications, for example, the sensing information can be converted to the microwave domain, thus increasing the

interrogation speed and resolution. This article reviews three FBG sensors with improved interrogation resolution and speed implemented based on microwave photonics techniques. The first technique is implemented based on spectral shaping and frequency-to-time mapping to convert a spectrum-shaped optical waveform to a chirped microwave waveform in which the sensing information is encoded in the chirped microwave waveform as a frequency shift. Through pulse compression, the frequency shift is obtained by estimating the location of the highly compressed correlation peak with significantly increased resolution. In the system, a linearly chirped FBG (LCFBG) is incorporated in one arm of a Mach–Zehnder interferometer (MZI). Thus, the MZI has a spectral response with an increasing free spectral range (FSR). An ultra-short pulse with a ultra-broad spectrum is spectrally shaped by the MZI and sent to a dispersive fiber for frequency-to-time mapping [6] to generate a linearly chirped microwave waveform. Through chirped microwave pulse compression [7], a technique widely used in modern radar systems to increase the range resolution, a correlation peak with the location containing the sensing information (wavelength shift) is obtained. The interrogation speed is in the order of megahertz. If a high-birefringence (Hi-Bi) LCFBG is used to replace the single-mode LCFBG, both strain and temperature information can be measured [8]. In the second approach, a tunable optoelectronic oscillator (OEO) [9] based on a phase-shifted FBG (PS-FBG) [10] is employed to conduct extremely fast FBG strain sensing [11]. In the OEO, a phase modulator (PM) and a PS-FBG form a high-Q bandpass microwave photonic filter (MPF) [12]. The central frequency of the MPF is changed by applying a strain to the PS-FBG, leading to a frequency shift in the oscillation signal. By measuring the frequency shift, the interrogation of the sensor is performed. The interrogation speed is in the order of megahertz. The resolution is determined by the mode spacing of the OEO. By increasing the loop length of the OEO, the mode spacing is reduced and the interrogation resolution is increased. In the experiment, an unprecedented resolution of 360 femtometer, a high signal-to-noise ratio (SNR) better than 70 dB, and a large frequency (wavelength) interrogation range over tens of gigahertz is demonstrated. In the third approach, a temperature-insensitive transverse load sensor based on a tunable dual-frequency OEO is implemented [13]. Instead of using a PS-FBG written in a single-mode fiber, a PS-FBG written in a Hi-Bi fiber is employed. Due to the birefringence of the Hi-Bi PS-FBG, a high-Q dual-bandpass MPF with two oscillation frequencies is produced. By incorporating the dual-bandpass MPF into the OEO, two oscillation frequencies are generated, which lead to the generation of a third frequency, which is the beat frequency between the two oscillation frequencies. Since the two oscillation frequencies experience the same temperature-induced frequency shift, the beat frequency is only sensitive to the transverse load. The transverse load sensor is experimentally demonstrated. The sensitivity and the minimal detectable load are measured to be as high as ~9.73 GHz/(N/mm) and 2.06×10^{-4} N/mm, respectively. The high-frequency purity and stability of the generated microwave signal by the OEO permit extremely reliable and high-accuracy measurement. The frequency interrogation allows the system to operate at an ultra-high speed. In what follows, the three FBG sensors are discussed in detail.

2. A Strain and Temperature Sensor with Improved SNR and Resolution

First discussed is an FBG sensor with both improved SNR and resolution, which is implemented based on spectral-shaping and frequency-to-time mapping [6, 14] to generate a linearly chirp microwave waveform containing the sensing information (wavelength shift) followed by pulse compression to extract the sensing information
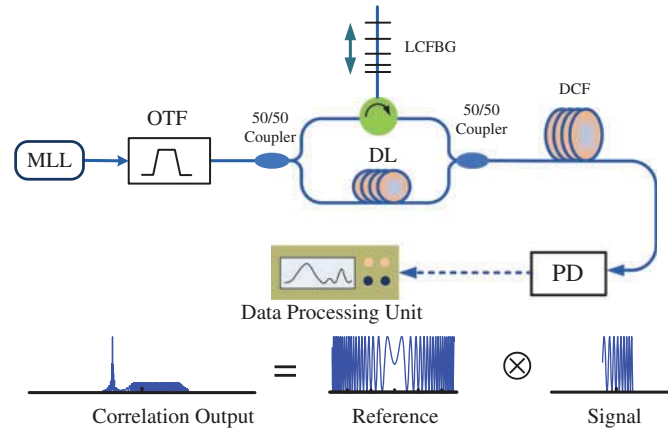
Figure 2. LCFBG sensor interrogation system based on spectral-shaping and frequency-to-time mapping (MLL: mode-locked laser; OTF: optical tunable filter).

[6, 8]. As shown in Figure 2, an LCFBG is incorporated in one arm of an MZI. Due to the wavelength-dependent nature of the length of the arm with the incorporated LCFBG, the MZI has a spectral response with an increasing FSR. An ultra-short optical pulse with a wide spectrum from a mode-locked laser source is spectrally shaped by the MZI, and the shaped spectrum is then mapped to the temporal domain by a dispersive device, which can be a dispersive fiber or an LCFBG. In the experiment, a dispersion compensating fiber (DCF) is used as the dispersive device. Due to the linear frequency-to-time mapping, a linearly chirped microwave waveform with a temporal shape that is a scaled version of the shaped spectrum is generated. The chirped waveform is detected by a photodetector (PD) and then sent to a digital signal processor to perform pulse compression.

It is known that a chirped waveform can be compressed if it is sent to a correlator or a matched filter in which a reference waveform that is identical to the chirped waveform is correlated with the generated chirped waveform. The key significance here is that the wavelength shift is estimated by measuring the location of the correlation peak, with both improved resolution and SNR. The correlation is done here by building a reference microwave waveform, which is linearly chirped with a chirp rate identical to that of the generated chirped microwave waveform but with an instantaneous frequency extending from the smallest to the largest possible values corresponding to the generated chirped microwave waveform when the LCFBG is experiencing the largest and the smallest wavelength shift. Therefore, the location of the correlation peak would indicate the wavelength shift.

Figure 3 shows the experimental results. A microwave waveform with a chirp rate of –0.068 GHz/ps for $t < 0$ and 0.068 GHz/ps for $t > 0$ is built as a reference microwave waveform, as shown in Figure 3a. Figures 3b, 3c, and 3d show three linearly chirped microwave waveforms corresponding to three strains of 71.5, 406.9, and 484.2 applied to the LCFBG, respectively. The correlation of the three linearly chirped microwave waveforms with the reference microwave waveform is shown in Figure 3e. The waveforms are highly compressed. The locations of the three peaks indicate the wavelength shifts of the LCFBG are 0.087, 0.495, and 0.589 nm, corresponding to three different strains of 71.5, 406.9, and 484.2 $\mu\varepsilon$, respectively.
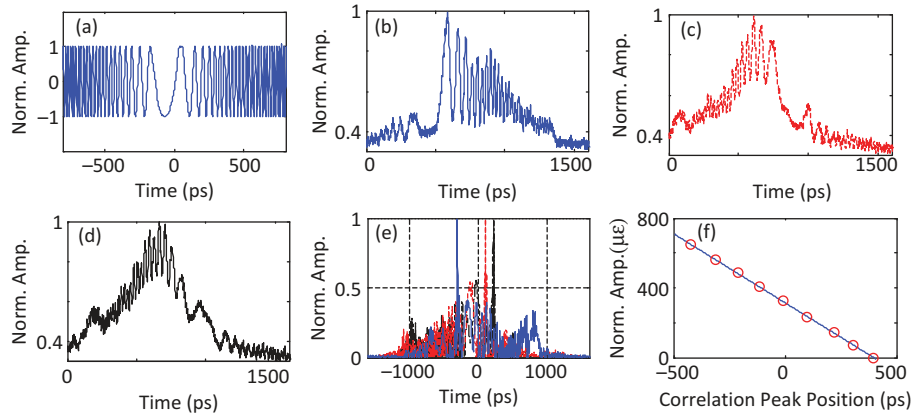
Figure 3. Experimental results: (a) reference microwave waveform; (b) measured chirped microwave waveform when a strain of 71.5 με is applied to the LCFBG; (c) measured chirped microwave waveform when a strain of 406.9 με is applied to the LCFBG; (d) measured chirped microwave waveform when a strain of 484.2 με is applied to the LCFBG; (e) correlation results for the detected microwave waveforms as show in (b), (c), and (d); (f) the measured strain versus the peak position. The circles are the experimental data, and the solid curve is linear fitting of the experimental data.
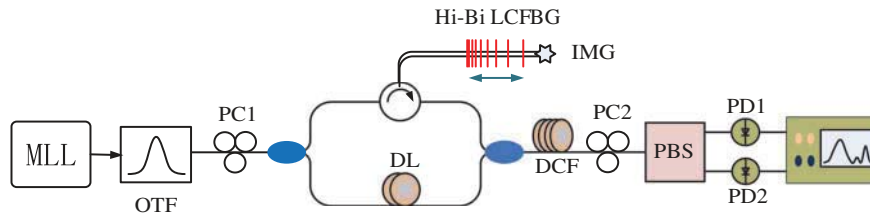

Figure 4. Schematic of a Hi-Fi LCFBG sensor interrogation system for simultaneous interrogation of temperature and strain (PBS: polarization beam splitter; IMG: index matching gel; OTF: optical tunable filter).

The system could also be improved for simultaneous interrogation of temperature and strain by changing the single-mode LCFBG to a Hi-Bi LCFBG, as shown in Figure 4. The strain and temperature information is encoded in the Hi-Bi LCFBG as Bragg wavelength shifts along the fast and slow axes. Due to the birefringence in the Hi-Bi LCFBG, the MZI has two spectral responses along the fast and slow axes with each having an increasing FSR. The spectrum of an ultra-short optical pulse is spectrally shaped by the MZI. Two spectrum-shaped signals are obtained at the output of the MZI, which are mapped to two chirped microwave waveforms by a dispersive fiber. Again, based on chirped microwave pulse compression, two correlation peaks with the locations containing the strain and temperature information are obtained.

The simultaneous temperature and strain measurements are experimentally demonstrated. Figure 5a shows the reference microwave waveform, and Figures 5b and 5c show two linearly chirped microwave waveforms corresponding to the polarization directions of the ultra-short pulse aligned with the fast axis and slow axis of the Hi-Bi LCFBG, respectively, when the strain is 50 με and the temperature is 25ºC. The correlation of the two linearly chirped microwave waveforms with the reference microwave waveform given
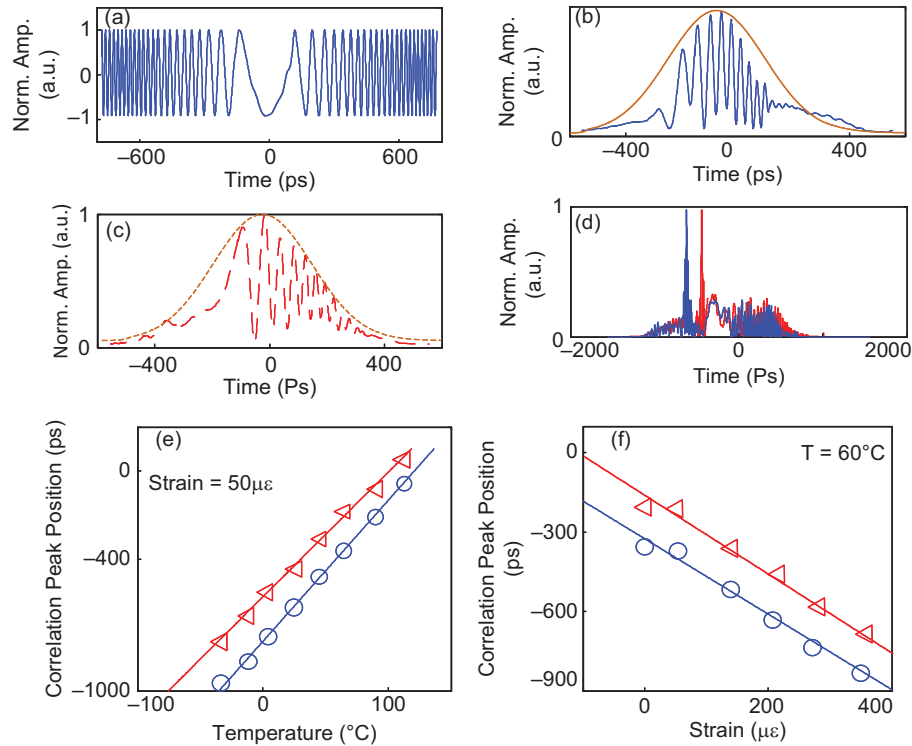
Figure 5. Experimental results: (a) reference microwave waveform; a linearly chirped microwave waveform corresponding to the polarization direction of the ultra-short pulse when a strain of 50 με is applied to the LCFBG at 25°C: (b) aligned with the fast axis and (c) aligned with the slow axis; (d) correlation of the waveforms shown in (b) and (c) with the special reference waveform; (e) correlation peak position versus the temperature for a given strain of 50 με; (f) correlation peak position versus the applied strain for a temperature of 60°C. The triangular and circles indicate the experimental data corresponding to the polarization direction of the ultra-short pulse aligned with the fast axis and slow axis, respectively.

in Figure 5a is shown in Figure 5d. It can be seen that the waveforms are highly compressed. The locations of the two peaks indicate the wavelength shifts of the Hi-Bi LCFBG and the phase difference due to the birefringence of the Hi-Bi fiber. In the experiment, the relationship between the strain, temperature, and the correlation peak positions is measured, which is shown in Figures 5e and 5f.

3. A Strain Sensor Based on a Tunable OEO Employing a PS-FBG

A high-resolution strain sensor can be implemented using a tunable OEO employing a PS-FBG. The schematic of an OEO-based strain sensor is shown in Figure 6a [11]. A light wave from a tunable laser source (TLS) is sent to a two-port PM through a polarization controller (PC). A phase-modulated light wave is generated at the output of the PM and is sent to a PS-FBG through an optical circulator (OC) and is then reflected by the PS-FBG. The reflected optical signal is sent to a PD. After electrical amplification by a power amplifier (PA), the output microwave signal from the PD is split into two microwave signals by a
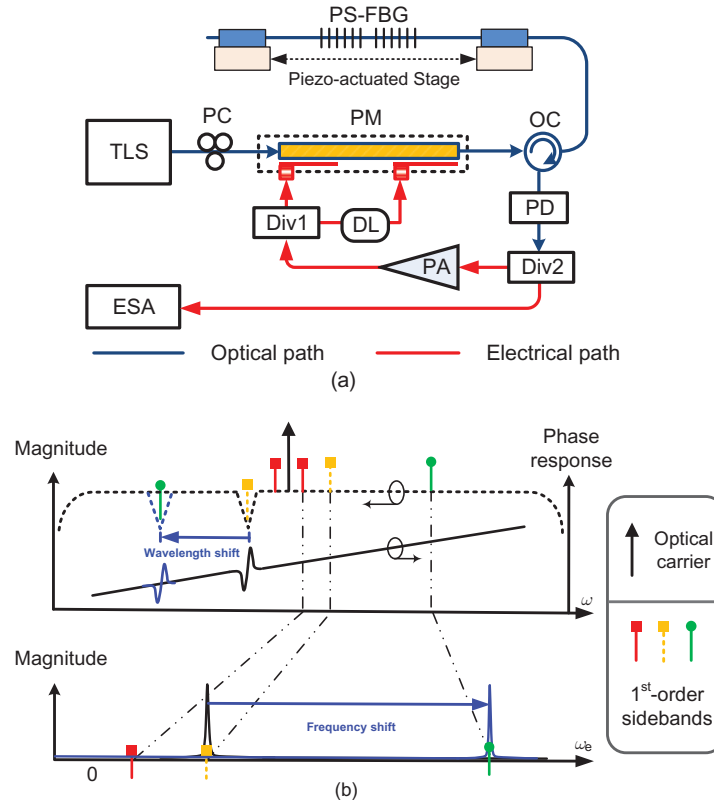
Figure 6. (a) A strain sensor based on a tunable OEO employing a single-mode PS-FBG and (b) implementation of the equivalent high-Q MPF. Upper: he magnitude and phase response of the PS-FBG; lower: frequency response of the MPF with different loaded strain.

power divider (Div1) and fed back to the PM via the two RF ports. The generated microwave signal at the output of the PD is also sent to an electrical spectrum analyzer (ESA) via a second power divider (Div2). The open-loop frequency response of the OEO corresponds to an ultra-high-Q MPF, realized based on phase-modulation to intensity-modulation conversion by filtering out one sideband of the phase-modulated signal using the ultra-narrow notch of the PS-FBG, with a width of only a few tens of megahertz. Note that a time delay difference between the two microwave signals applied to the two ports of the PM is introduced by a delay line (DL) to form a two-tap microwave delay-line filter to reduce further the bandwidth of the MPF. As shown in Figure 6b, when the PS-FBG is stretched, the resonance wavelength is shifted due to the change of the grating pitch. As a result, the central frequency of the MPF is accordingly shifted. The OEO translates the wavelength-domain measurement into an electrical spectrum measurement, thus ensuring a significantly higher frequency resolution. The wavelength resolution is limited by the frequency spacing of the oscillating modes in the OEO. In addition, the use of an oscillation scheme also has a very positive impact on the measurement SNR performance.

Figure 7 shows the experimental results. The PS-FBG was fabricated by introducing a π phase shift to the grating during the FBG fabrication process. In the experiment, the PS-FBG was mounted on a piezo-actuated stage. The central wavelength of the ultra-narrow notch is
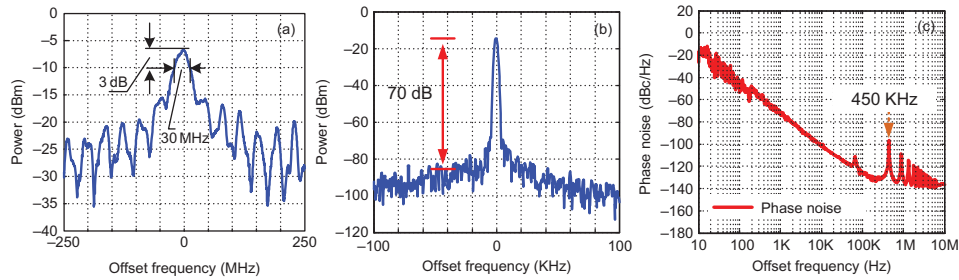
Figure 7. (a) Measured frequency response of the PS-FBG-based MPF, (b) spectrum of the 10-GHz microwave signal generated by the OEO, and (c) phase noise of the generated 10-GHz microwave signal.

about 1,549.28 nm, with a full-width at half-maximum (FWHM) width of about 30 MHz, which determines the bandwidth of the equivalent MPF of the open-loop OEO, as shown in Figure 7a. When the OEO loop is closed, a microwave signal with a frequency at 10 GHz and a 70-dB sidemode suppression ratio (SMSR) is generated, as shown in Figure 7b. Since the noise level is below the level of the highest sidemode, the detection capability of the OEO sensor is only limited by the SMSR, which is 70 dB, well beyond the achievable values by any other techniques. The phase noise performance of the generated 10-GHz microwave signals is given in Figure 7c. Several peaks are observed for offset frequencies equal to or greater than 450 kHz. Thus, this frequency (450 kHz) corresponds to the longitudinal mode spacing of the OEO. When the resonance wavelength of the PS-FBG is shifted due to the applied strain with a frequency (wavelength) spacing >450 kHz (or equivalently >360 fm), the frequency of the generated microwave signal is then accordingly shifted and can be easily measured using an ESA. Figure 8a shows the measured frequency response of the PS-FBG-based MPF for different applied axial strains. The spectra of the generated microwave signals at the OEO output corresponding to the different applied strains are shown in Figure 8b. The frequency of the generated microwave signal is shifted from about 7 to 17 GHz. The maximum frequency is limited by the operation bandwidths of the microwave and optoelectronic components. The measurements confirm the expected linear relationship between the applied strain and the frequency of the generated microwave signal, as shown in Figure 8c.
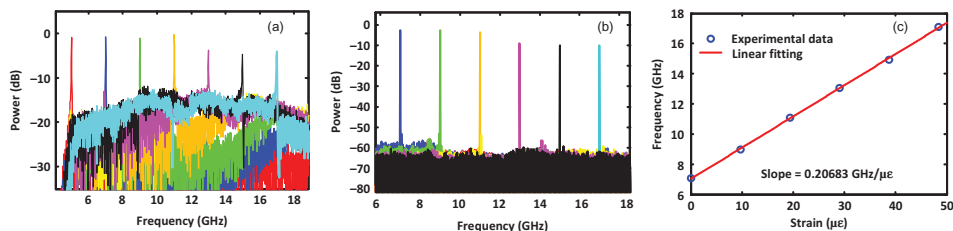

Figure 8. (a) Measured frequency response of the PS-FBG-based MPF for different applied strains, (b) spectra of the generated microwave signal at the OEO output for different strains, and (c) relationship between the applied strain and the frequency of the generated microwave signal.

4. A Temperature-Insensitive Transverse Load Sensor Based on a Dual-Frequency OEO Employing a Hi-Bi PS-FBG

A temperature-insensitive transverse load sensor can be implemented based on a dual-frequency OEO employing a Hi-Bi PS-FBG [13]. Figure 9 shows the configuration. A light wave generated by a laser diode (LD) is sent to a polarization modulator (PolM) via a PC (PC1). The PolM is a special PM that supports phase modulation along the orthogonal principal axes with complementary phase modulation indices. If the polarization direction of the incident light wave is aligned with one of the principal axes, the PolM operates as a regular PM. The phase-modulated signal is then sent to the Hi-Bi PS-FBG through an OC. One sideband of the phase-modulated signal is filtered out by the notch of the Hi-Bi PS-FBG, and the phase-modulated signal is converted to a single-sideband intensity-modulated (SSB-IM) signal and is detected at a PD. The detected electrical signal is sent back to the PolM after amplification by an electrical amplifier (EA) to close the OEO loop. The entire operation is equivalent to an MPF, with the central frequency of the passband determined by the wavelength spacing between the optical carrier and the notch wavelength.

Figure 10a shows the passband of the MPF along the horizontal or vertical polarization direction, measured by aligning the polarization of the incident light wave having an angle of 0° or 90° relative to one principal axis of the PolM. When the polarization of the
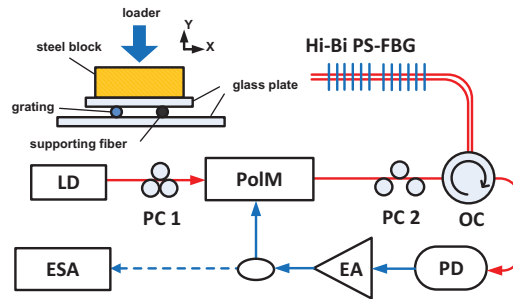

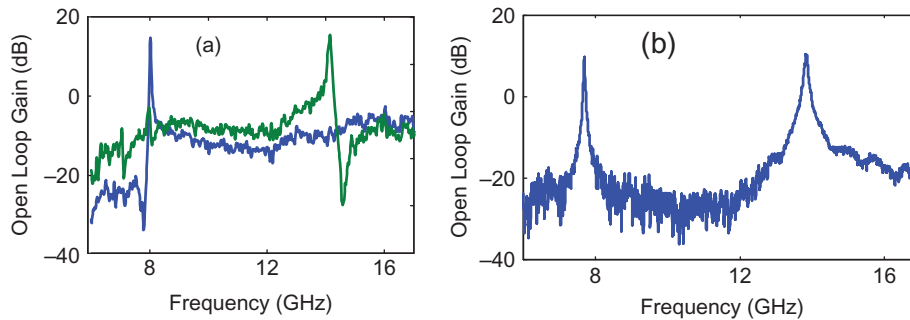**Figure 9.** Transverse load sensor based on a dual-frequency OEO.

Figure 10. (a) Single passband photonic microwave filter when the polarization of the incident light wave is alighted with an angle of 0° or 90° relative to one principal axis of the PolM and (b) dual passband photonic microwave filter when the polarization of the incident light wave is alighted with an angle of 45° relative to one principal axis of the PolM.
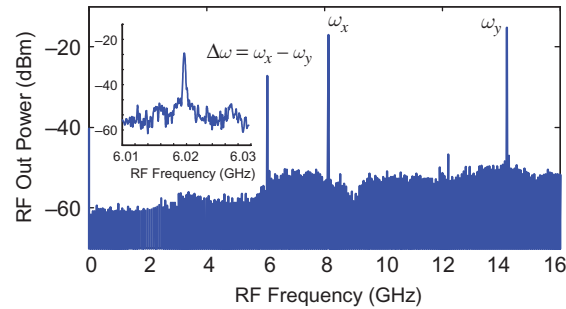
Figure 11. Electrical spectrum of the signal generated by the dual-frequency OEO with two microwave signals at 8.22 and 14.24 GHz and a beat signal at 6.02 GHz.

incident light wave is aligned with an angle of 45° relative to one principal axis of the PolM, the light wave is equally projected to the two orthogonal polarization axes; thus, a photonic microwave filter with two passbands is implemented. Figure 10b shows the filter response when the polarization of the incident light wave is aligned with an angle of 45° relative to one principal axis of the PolM. A dual passband filter is realized. When the OEO loop is closed, two microwave signals at two frequencies determined by the two passbands are generated. If a load is applied to the Hi-Bi PS-FBG, the central frequencies of the two passbands will be shifted, and the corresponding oscillation frequencies of the microwave signals will also be shifted. Due to the non-linearity of the PolM, a third frequency corresponding to the beat signal between the two microwave signals is also generated, as shown in Figure 11. Since the two oscillation frequencies experience an identical frequency shift due to temperature change, the frequency of the beat note is only associated with the birefringence introduced by the transverse load to the PS-FBG. Thus, by measuring the beat frequency, the transverse load is measured.

If a transverse load is applied to the Hi-Bi PS-FBG, a change in the beat frequency corresponding to the applied transverse load is generated. To ensure the system reaches its highest sensitivity and to have a good linearity between the transverse load and the beat frequency, in the experiment the transverse load is applied to the Hi-Bi PS-FBG along the fast axis. A supporting fiber with an identical radius is placed in parallel with the PS-FBG to make the load is applied to the Hi-Bi PS-FBG transverse while sharing half of the applied load. By increasing the load applied to the PS-FBG, the beating frequency is shifted linearly toward a smaller frequency, as shown in Figure 12. The spectrum of the beat signal is measured by an ESA, with the spectrum shown in the inset of Figure 12. By using the typical values of a silica fiber, one obtains the relationship between the transverse load and beat frequency, given by $dv/dF \approx 9.9\,\text{GHz}/(\text{N/mm})$ [15]. The slope through linear fitting is –9.73 GHz/(N/mm), which agrees well with the theoretical value of 9.9 GHz/(N/mm).

5. Discussions

The key to achieving a high interrogation resolution and speed of an FBG sensor is to convert the spectral information (wavelength shift) to the time domain, and the spectral information is extracted using a digital signal processor at a much faster speed. Table 1 shows a comparison of the performance of the proposed techniques based on microwave photonics with other
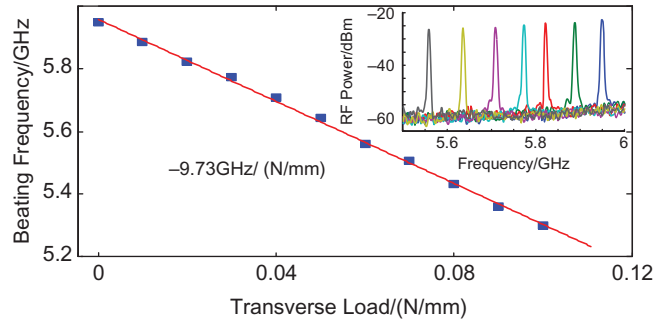
Figure 12. Measured beat frequency as a function of the transverse load and the electrical spectrum with different load.

Table 1

Comparison of the performance of the interrogation based on microwave photonics with other conventional FBG interrogation techniques

Interrogation techniques	Optical spectrum analyzer	Edge filter	Scanning FP filter	Wavelength-to-time mapping	Optoelectronic oscilloscope
Interrogation speed	1 Hz	100 kHz	1 kHz	10 MHz	10 MHz
Interrogation resolution (pm)	10	10	1	0.25	0.36

conventional FBG interrogation techniques. As can be seen, both the interrogation speed and the resolution are significantly increased as compared with conventional techniques using an optical spectrum analyzer, an optical edge filter, and a scanning FP filter.

6. Conclusion

Three different FBG sensors implemented based on microwave photonics techniques to increase the interrogation speed and sensing resolution were reviewed. In the first FBG sensor, spectral-shaping and frequency-to-time mapping to convert a spectrally shaped optical spectrum to a linearly chirped microwave waveform were employed. By using chirped pulse compression, an FBG sensor with high speed (in MHz) and high resolution was implemented. The spectrally shaped optical spectrum was generated by passing an optical pulse through an MZI incorporating an LCFBG to have linearly decreasing FSR. If the regular PS-FBG was replaced by a Hi-Bi PS-FBG, two chirped microwave waveforms were generated and simultaneous strain and temperature measurements could be achieved. In the second FBG sensor, a tunable OEO incorporating a single-mode PS-FBG was used, which provided an ultra-high resolution and fast interrogation by measuring the oscillation frequency. In the third FBG sensor, a dual-frequency OEO incorporating a Hi-Bi PS-FBG to measure a transverse load was demonstrated. Fast interrogation was also achieved by measuring a third frequency, which was the beat frequency between the two microwave frequencies due to the

birefringence of the Hi-Bi PS-FBG, which was temperature insensitive. The sensitivity and the minimal detectable load were measured to be as high as –9.73 GHz/(N/mm) and 2.06×10^{-4} N/mm, respectively.

Acknowledgments

Funding

References

1. Othonos, A., and Kalli, K. 1999. *Fiber Bragg Gratings: Fundamentals and Applications in Telecommunications and Sensing*. Norwood: Artech House.
2. Cavaleiro, P. M., Araujo, F. M., Ferreira, L. A., Santos, J. L., and Farahi, F. 1999. Simultaneous measurement of strain and temperature using Bragg gratings written in germanosilicate and Boron-codoped germanosilicate fibers. *IEEE Photonics Technology Letters* 11(12):1635–1637.
3. James, S. W., Dockney, M. L., and Tatam, R. P. 1996. Simultaneous independent temperature and strain measurement using in-fiber Bragg grating sensors. *Electronics Letters* 32(12):1133–1134.
4. Patrick, H. J., Williams, G. M., Kersey, A. D., Pedrazzani, J. R., and Vengsarkar, A. M. 1996. Hybrid fiber Bragg grating/long period fiber grating sensor for strain and/temperature discrimination. *IEEE Photonics Technology Letters* 8(9):1223–1223.
5. Miao, Y., Liu, B., and Zhao, Q. 2008. Simultaneous measurement of strain and temperature using single tilted fibre Bragg grating. Electronics Letters 44(21):1242–1243.
6. Wang, C., and Yao, J. P. 2008. Photonic generation of chirped millimeter-wave pulses based on nonlinear frequency-to-time mapping in a nonlinearly chirped fiber Bragg grating. *IEEE Transactions on Microwave Theory Technology* 56(2):542–553.
7. Liu, W., Li, M., Wang, C., and Yao, J. P. 2011. Real-time interrogation of a linearly chirped fiber Bragg grating sensor based on chirped pulse compression with improved resolution and signal-to-noise ratio. *Journal of Lightwave Technology* 29(9):1239–1247.
8. Liu, W., Li, W., and Yao, J. P. 2011. Real-time interrogation of a linearly chirped fiber Bragg grating sensor for simultaneous measurement of strain and temperature. *IEEE Photonics Technology Letters* 23(18):1340–1342.
9. Li, W., and Yao, J. P. 2012. A wideband frequency-tunable optoelectronic oscillator incorporating a tunable microwave-photonic filter based on phase-modulation to intensity-modulation conversion using a phase-shifted fiber Bragg grating. *IEEE Transactions on Microwave Theory Technology* 60(6):1735–1742.
10. Erdogan, T. 1997. Fiber grating spectra. *Journal of Lightwave Technology* 15(8):1277, 1294.
11. Li, M., Li, W., Yao, J., and Azana, J. 2012. Femtometer-resolution wavelength interrogation of a phase-shifted fiber Bragg grating sensor using an optoelectronic oscillator. *OSA Topical Meeting on Bragg Gratings, Photosensitivity, and Poling in Glass Waveguides*, Colorado Springs, CO, June 17–21, Paper BTu2E.3.
12. Li, W., Li, M., and Yao, J. P. 2012. A narrow-passband and frequency-tunable micro-wave photonic filter based on phase-modulation to intensity-modulation conversion using a phase-shifted fiber Bragg grating. *IEEE Transactions of Microwave Theory Technology* 60(5): 1287–1296.

13. Kong, F., Li, W., and Yao, J. P. 2013. Transverse load sensing based on a dual-frequency optoelectronic oscillator. *Optics Letters* 38(14):2611–2613.
14. Yao, J. P. 2011. Photonic generation of microwave arbitrary waveforms. *Optics Communications* 284(15):3723–3736.
15. Guan, B. O., Jin, L., Zhang, Y., and Tam, H. Y. 2012. Polarimetric heterodyning fiber grating laser sensors. *Journal of Lightwave Technology* 30(8):1097–1112.

Biography

Jianping Yao is a Professor and University Research Chair in the School of Electrical Engineering and Computer Science, University of Ottawa, Canada. Prof. Yao has published over 480 papers in refereed journals and conference proceedings. He is a topical editor for *Optics Letters*, and serves on the Editorial Boards of *Optics Communications* and *Science Bulletin*. Prof. Yao is a Fellow of IEEE, a Fellow of the Optical Society of America, and a Fellow of the Canadian Academy of Engineering.